Biophysical Chemistry 13 (1981) 105–116
North-Holland Publishing Company

MOLECULAR DYNAMICS STUDY OF ION TRANSPORT IN TRANSMEMBRANE PROTEIN CHANNELS

W. FISCHER, J. BRICKMANN *
Physikalische Chemie I, Technische Hochschule Darmstadt, D-6100 Darmstadt, FRG

and

P. LÄUGER
Fakultät für Biologie, Universität Konstanz, D-7750 Konstanz, FRG

Received 27 August 1980

Ion transport through biological membranes often takes place via pore-like protein channels. The elementary process of this transport can be described as a motion of the ion in a quasi-periodic multi-well potential. In this study molecular dynamics simulations of ion transport in a model channel were performed in order to test the validity of reaction-rate theory for this process. The channel is modelled as a hexagonal helix of infinite length, and the ligand groups interacting with the ion are represented by dipoles lining the central hole of the channel. The dipoles interact electrostatically with each other and are allowed to oscillate around an equilibrium orientation. The coupled equations of motion for the ion and the dipoles were solved simultaneously with the aid of a numerical integration procedure. From the calculated ion trajectories it is seen that, particularly at low temperatures, the ion oscillates back and forth in the trapping site many times before it leaves the site and jumps over the barrier. The observed oscillation frequency was found to be virtually temperature-independent ($\nu_0 \approx 2 \times 10^{12}$ s^{-1}) so that the strong increase of transport rate with temperature results almost exclusively from the Arrhenius-type exponential dependence of jump probability w on $1/T$. At higher temperatures simultaneous jumps over several barriers occasionally occur. Although the exponential form of $w(T)$ was in agreement with the predictions of rate theory, the activation energy E_a as determined from $w(T)$ was different from the barrier height which was calculated from the static potential of the ion in the channel; the actual transport rate was 1×10^3 times higher than the rate predicted from the calculated barrier height. This observation was interpreted by the notion that ion transport in the channel is strongly influenced by thermal fluctuations in the conformation of the ligand system which in turn give rise to fluctuations of barrier height.

1. Introduction

Ion transport across biological membrane occurs by special mechanisms different from simple diffusion through the lipid bilayer. An important transport mechanism is the passage of ions through localized structures called channels [1]. An ion channel may be a built-in protein that offers to the ion an energetically favourable pathway through the apolar core of the membrane. A well-characterized example is the cation-permeable channel formed by gramicidin A [2–7], a linear peptide consisting of mostly hydrophobic amino acids. The gramicidin channel has a helical structure with a central tunnel of about 4 Å in diameter running along the helix axis. An ion passing through the channel may interact with the oxygen atoms of the peptide carbonyl groups lining the wall of the tunnel. In this way the carbonyls act as ligands which replace part of the primary hydration shell surrounding the ion in water. It is likely that during the passage of the cation the channel structure is transiently distorted in such a way that the carbonyl groups are tilted with their oxygen ends towards the ion [2]. Small univalent cations may pass through the gramicidin channel at a

* Author to whom correspondence should be addressed.

0 301–4622/81/0000–0000/$ 2.50

rate of up to 10^7-10^8 s^{-1} [3] which is similar to the transport rate of Na^+ in the sodium channel of nerve membranes [8].

An important goal in the study of ion channels is a better understanding of the relationship between the observable transport properties and the microscopic parameters of the channel (geometry of the ligand system, interaction energy between ion and ligand groups, force constants governing the deformation of the peptide backbone, and so on). For the theoretical description of ion permeation through channels the pathway of the ion may be represented as a sequence of energy wells which are the sites where the ion is in an energetically favourable interaction with one or several ligand groups. Ion movement in the channel may then be visualized as a series of thermally activated jumps over the energy barriers separating the trapping sites [15–18]. Using rate-theory analysis, the frequency of jumps over a barrier is obtained as a frequency factor times the exponential of an activation energy. While this approach leads to a qualitatively correct description, the existing treatments are still unsatisfactory in two respects. In the application of rate-theory to ion permeation, the barrier structure of the channel is usually assumed to be fixed, i.e., independent of time and independent of the movement of the ion. This description which corresponds to an essentially static picture of protein structure does not allow for the fact that the ligands system itself is subjected to thermal fluctuations and, furthermore, that it may be distorted by the movement of the ion [31]. A second problem in the application of rate-theory to transport processes consists in the fact that it is difficult to test the theory rigorously. A complete comparison between theory and experiment requires independent experimental information on both transport rates and barrier energies. This condition, however, is rarely met, and usually it is only possible to infer barrier heights from measured transport rates, assuming that the theoretical expressions relating both quantities are correct.

In recent years the method of molecular dynamics has been widely used as a powerful technique for predicting macroscopically observable properties from the microscopic parameters of a system [9–11]. Starting with a set of initial conditions, the time behaviour of a system of many interacting particles is calculated by explicit numerical integration of the coupled Newtonian equations of motion. This method has been used to study diffusion in liquids and also to analyze permeation of molecules through rigid membrane pores [12,13].

In this communication we present results from a molecular dynamics study of ion transport through a model channel. The ligand system is modelled as a helical array of dipoles lining the central hole of the channel. The dipoles interact electrostatically with each other and with the permeating ion moving along the helix axis, and each dipole is allowed to oscillate around an equilibrium orientation with respect to the helix axis. By computer simulation of this dynamical system the trajectory of the ion in the channel is calculated, and from the trajectory the mean jump rate of the ion over the barriers is obtained. Performing such analyses at different temperatures yields the activation energy of transport which may be compared with the static value of the barrier height. In this way the influence of barrier fluctuations on transport rates may be studied and, at the same time, the predictions of rate-theory analysis may be tested under a variety of conditions.

2. Description of the model

In this work the protein channel is modelled by an infinite hexagonal rigid helix with radius r and six flexible groups per single helix turn located at its surface (fig. 1). The polar groups are represented by rigid dipoles with the positive pole (with effective charge q) fixed on the helix chain while the negative charge is allowed to move on a circle with fixed radius d towards the axis of the channel. The undistorted motion of the helix dipoles is then described by a torsional vibration with an equilibrium angle ϕ_i^0 of the ith dipole axis with respect to the radius of the helix. In fig. 2a a schematical representation of the equilibrium orientations of the dipoles is drawn for a model with all $\phi_i^0 = 70°$ while for the system shown in fig. 3a the equilibrium orientation alternates between $\phi_{2i}^0 = 70°$ and $\phi_{2i+1}^0 = -70°$. The dipoles are numbered according to their occurrence in the chain. The antiparallel orientation of dipoles in fig. 3a corresponds to the arrangement of the $C=O$ groups in the Gramicidin A channel [2]. The interaction of the polar ligands is described by dipole–dipole forces. This nonharmonic

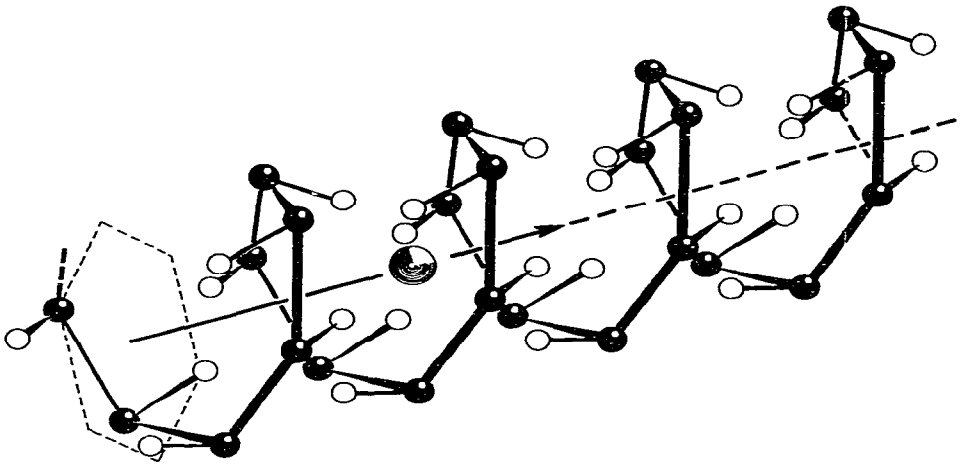

Fig. 1. Model of the protein channel. Dipoles are fixed with their positive poles (dark spheres) on a rigid hexagonal helix. Six dipoles are arranged per single turn. The negative poles (white spheres) are allowed to oscillate towards the axis of the helix. The permeating cation is constrained to move on the helix axis.

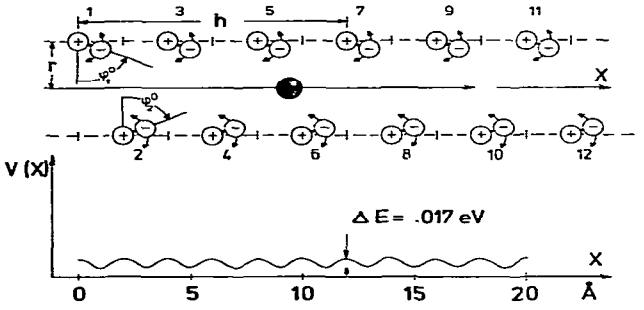

Fig. 2. a). Arrangement of the dipoles on the helix in model I (parallel orientation): all dipoles have the same equilibrium angle ϕ_i^0 with respect to ion-migration coordinate x; r is the radius of the helix and h the length per turn. For ease of representation, dipoles are depicted alternately on two lines parallel to the helix axis. b). Static potential energy $V(x)$ of the migrating ion resulting from Coulombic interaction with the dipoles. The dipoles are held fixed in the equilibrium orientation which is obtained for $T \to 0$ under the combined influence of the Coulombic dipole-dipole interaction and torsional forces. $\phi_i^0 = 70°$; $D_T = 1.08 \times 10^{-18}$ J; $r = 2.5$ Å; $h = 12$ Å; charge of the ion: $Q = e_0 = 4.803 \times 10^{-10}$ e.s.u. (e_0 is the elementary charge); charge of the dipole: $q = 0.25\ e_0$; length of the dipole: $d = 1.128$ Å.

coupling guarantees a rapid energy flow if the system of dipoles is allowed to perform oscillations according to the classical equations of motion.

The positive ion (charge Q) migrates through the channel in the field of the dipoles. In the present model the ion was constrained to move along the x axis of the helix (fig. 1), i.e., its motion can be described in a pseudo one-dimensional picture. The potential energy $V(x)$ for a univalent ion ($Q = e_0$, where e_0 is the elementary charge) as a function of the migration coordinate x is shown in figs. 2b and 3b for the case where the dipoles are held fixed in their equilibrium positions (i.e. in the orientation which is assumed under the combined influence of the Coulombic dipole–dipole interaction and the torsional force). If the dipoles are arranged in such a way that all axes are oriented towards the positive x-direction (model I with $\phi_i^0 = 70°$ for all i), $V(x)$ is a multi-well potential (see fig. 2b) with a very low barrier energy of $\Delta E = 0.017$ eV for a dipolar charge of $q = 0.25\ e_0$ and a dipolar length of $d = 1.128$ Å). The situation is totally changed (see discussion in section 5) if the orientation of polar groups alternates along the helix chain (model II, fig. 3b). Now the potential barriers increase by a factor of about 20 to give $\Delta E = 0.350$ eV. Moreover, model II contains only half the number of wells in the potential

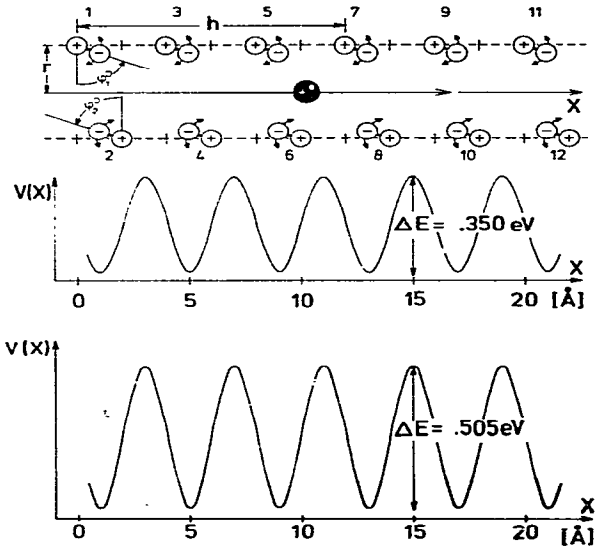

Fig. 3. a). Arrangement of the dipoles in model II (antiparallel orientation): the equilibrium orientation of the dipole axes alternates along the chain. b). Static potential $V(x)$ of the ion, calculated with the dipoles fixed in the equilibrium orientation which is obtained for $T \to 0$ under the same conditions as in fig. 2b, but with alternating values of $\phi_i^0 = \pm 70°$. All other parameter values are identical to those of fig. 2b. c). Adiabatic potential $V(x)$ of the ion: For each position x of the ion the system of dipoles was allowed to move to its potentials energy minimum (including torsional restoring forces, dipole–dipole and ion–dipole interactions). Torsional force constant $D_\tau = 1.08 \times 10^{-18}$ J; other parameter values as in fig. 2b.

energy, as compared with model I. In this study molecular dynamics calculations of ion migration along the helix axis were performed using model II since in model I no "trapping" of the ion in the model channel is to be expected.

3. Molecular dynamics simulation technique

In the molecular dynamics method the classical equations of motion

$$\dot{q}_i = \partial H/\partial p_i, \qquad \dot{p}_i = -\partial H/\partial q_i \tag{1}$$

are solved numerically, where (q_i, p_i) are pairs of canonically conjugated position and momentum variables and H is the total hamiltonian of the system. As usual, the dot indicates differentiation with respect to time. In our model each particle has only one degree of freedom. The ion can migrate along the coordinate x while the dipoles can only rotate with respect to a fixed axis with their negative charge held at a constant radius d. The possible inter-particle distances which influence the actual force on the particles are shown in fig. 4. x_i^0 is the x-coordinate of the fixed positive charge of the ith dipole, r_1^i, r_2^i, R_1^{ij}, and R_2^{ij} indicate distances between dipole charges and the ion and between charges of different dipoles, respectively, while ϕ_i is the angle of the dipole axis with respect to the radial direction of the channel. In our model the equations of motion for the ion [eq. (1)] have the following form:

$$\dot{x} = v, \qquad \dot{v} = -M^{-1}\partial V(x, x_i)/\partial x \tag{2}$$

with the potential energy

$$V(x, x_i) = V_M(x) + qQ \sum_j (1/r_2^j - 1/r_1^j), \tag{3}$$

v and M are the velocity and the mass of the ion, respectively, and $V_M(x)$ is an external potential which may result from an electrical field. For the dipole with number i one obtains in an analogous manner

$$\dot{\phi}_i = \omega_i, \qquad \dot{\omega}_i = -(md^2)^{-1}\partial V_i/\partial\phi_i \tag{4}$$

with

$$V_i = D_\tau(\phi_i - \phi_i^0)^2/2$$

$$+ q^2 \sum_{j \neq i} (1/R_1^{ij} - 1/R_2^{ij}) + qQ(1/r_2^i - 1/r_1^i). \tag{5}$$

Here m is the mass of the flexible part of the polar

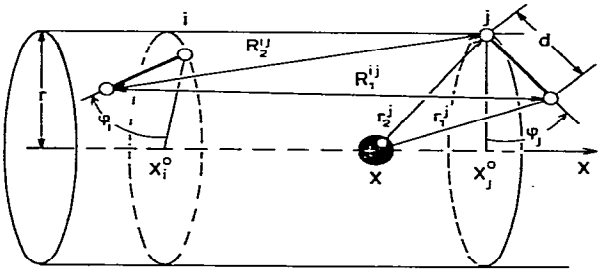

Fig. 4. Coordinates describing the interactions between the migrating cation at position x and two dipoles i and j.

ligand, ω_i is the angular velocity for the orientational motion of the dipole, and D_r is the force constant for the unperturbed dipole oscillation.

The force constant D_r and the mass m were chosen so that the oscillation frequency $\omega = (D_r/m)^{1/2}/d$ of the isolated dipole corresponds to a wavenumber of $\tilde{\nu} = 150\ \mathrm{cm}^{-1}$ which is of the order of magnitude of the skeletal deformation vibrations in peptides [14]. In order to account for the participation of adjacent parts of the peptide backbone in the bending motion, m was treated as an effective mass and was taken to be four times the mass of the oxygen atom ($m = 1.06 \times 10^{-22}$ g); accordingly, D_r was chosen to be 1.08×10^{-18} J. For d the length of the C=O bond was used ($d = 1.128$ Å) and for M the mass of a sodium ion ($M = 3.82 \times 10^{-23}$ g). Furthermore, the charges of the ion and the dipole were taken to be $Q = e_0 = 4.803 \times 10^{-10}$ e.s.u. and $q = 0.25\ e_0$. As usual in many molecular simulations of macroscopic properties we used periodic boundary condition in our numerical treatments. We solved the system of differential equations [eqs. (2) and (4)] simultaneously with the aid of the Runge-Kutta-integration scheme with a time step of $\Delta t = 2.5 \times 10^{-15}$ s. 50 000–100 000 time steps were carried out in each single calculation, corresponding to an integration time of about 7–14 h on the PDP 11/60 computer. The unit cell was chosen to contain 30 dipoles, i.e., the ligand motion is periodic after five turns of the pore helix. The system of dipoles was "thermalized" to a temperature T by the choice of proper initial conditions of the angular velocities ω_i. The total energy of the system (channel dipoles plus ion) was then stable during each calculation series, i.e. the total system represents a microcanonical ensemble.

4. Calculation of the ion diffusion coefficient

One of the main reasons for undertaking the present study was to test the validity of rate-theory analysis for the description of ion transport in channels [15–18]. If the diffusion of the ion takes place according to a trapping mechanism between different quasi-equilibrium sites in the channel, the diffusion coefficient D can be obtained from the distance a of adjacent sites and the one-sided hopping frequency ν in the absence of external forces [19]:

$$D = a^2 \nu. \tag{6}$$

This expression was used to determine the diffusion coefficient from the molecular dynamics results. In model II the hopping distance is $a = h/3 = 4$ Å. The frequency ν may be represented by

$$\nu = \nu_0 w. \tag{7}$$

Here ν_0 is the oscillation frequency of the ion in a trapping site as obtained from the simulation of the dynamical system, while

$$w = N_{\mathrm{jump}}/N \tag{8}$$

is the jump probability which can be obtained from the number of jumps, N_{jump}, in a single calculation series and the number N of attempts. N is twice the number of oscillations of the ion, since during one oscillation period the ion can migrate forward and backward and thus has two chances to leave a trapping site. The oscillation frequency of the ion was found to be $\nu_0 = 2.2 \times 10^{12}\ \mathrm{s}^{-1}$, independent of the initial conditions of the simulation which specify the temperature, so that the diffusion coefficient in our model is directly proportional to the jump probability w.

For an estimate of the error Δw in the numerical calculation of w we used the variance [20]

$$\sigma^2 = Nw(1 - w) \tag{9}$$

of binomial distribution; this yields

$$\Delta w = \sigma/N = [w(1 - w)]^{1/2} N^{-1/2}. \tag{10}$$

This formula is only approximately correct since the different trials of the ion to leave a trapping site cannot be considered as strictly independent. It is well known from experimental observations that most activated rate processes like hopping diffusion in condensed matter follow the Arrhenius temperature dependence

$$\nu = D/a^2 = A(T) \exp(-E_a/kT). \tag{11}$$

where k is Boltzmann's constant, E_a is the activation energy, and $A(T)$ is a preexponential factor which may be weakly temperature dependent. There is no a priori relation valid for all activated rate processes between the activation energy E_a and microscopic parameters like the height of the potential barrier V_0 separating the energy wells. Moreover, the temperature dependence of the preexponential factor $A(T)$ differs qualitatively in different experimental situations. Various theo-

retical concepts have been developed to calculate the rate constant ν from microscopical parameters. In Eyring's formulation of the absolute reaction rate theory [21–24] the rate constant of a thermally activated rate process is given by the expressions

$$\nu = (kT/h)\Omega^{\ddagger}\Omega^{-1}\kappa \exp(-V_0/kT) \tag{12}$$

$$= (kT/h)\kappa \exp(\Delta\bar{S}^{\ddagger}/R)\exp(-\Delta\bar{H}^{\ddagger}/RT) \tag{13}$$

$$= (kT/h)\kappa \exp(-\Delta\bar{G}^{\ddagger}/RT), \tag{14}$$

where h is Planck's constant, $\Omega^{\ddagger}$ and Ω are the partition functions of the "activated state" and the "normal state" respectively. κ is a dimensionless transmission coefficient, with $1/2 < \kappa < 1$ for classical models [30] and V_0 is the height of the activation barrier. $\Delta\bar{S}^{\ddagger}$, $\Delta\bar{H}^{\ddagger}$, and $\Delta\bar{G}^{\ddagger}$ are the molar entropy, enthalpy and Gibbs free energy changes respectively, required to promote the migrating particles into the activated state. In the Eyring expression [eq. (12)] the preexponential factor $(kT/h)\Omega^{\ddagger}\Omega^{-1}$ can be further simplified using the partition functions $\Omega^{\ddagger}$ and Ω in the harmonic approximation and assuming that the vibrational frequencies ν_i perpendicular to the reaction coordinate are the same in the quasi-equilibrium and transition state. Thus,

$$\Omega^{\ddagger} = \prod_{i=1}^{f-1} \Omega_i, \quad \Omega = \Omega_0\Omega^{\ddagger}. \tag{15}$$

Ω_0 is the partition function of vibration along the diffusion coordinate. The quantum mechanical form of the vibrational partition functions is given by [24]

$$\Omega_i = \exp(-\Theta_i/2T)[1 - \exp(-\Theta_i/T)]^{-1} \tag{16}$$

where $\Theta_i = h\nu_i/k$ and $i = 0, 1, 2, \ldots, f-1$. With eqs. (15) and (16) one obtains

$$\nu = (kT/h)\Omega_0^{-1} \exp(-V_0/kT) = \nu_0(T/\Theta_0)$$

$$\times [1 - \exp(-\Theta_0/T)] \exp[-(V_0 - h\nu_0/2)/kT] \tag{17}$$

and the activation energy becomes

$$E_a = V_0 - h\nu_0/2. \tag{18}$$

In the high temperature range ($T > \Theta_0$) the preexponential factor can be simplified using the linear expansion $1 - \exp(-\Theta_0/T) \approx \Theta_0/T$, and the rate becomes

$$\nu = \nu_0 \exp(-E_a/kT), \tag{19}$$

while for low temperature ($T < \Theta_0$) the preexponential factor is linear in T:

$$\nu = \nu_0(T/\Theta_0) \exp(-E_a/kT)$$

$$= (kT/h) \exp(-E_a/kT). \tag{20}$$

In the present case a value of $\Theta_0 = 103.2$ K is obtained from the dynamically determined oscillation frequency ν_0 (practically independent of temperature, see fig. 5). Thus, the approximate relation eq. (19) for the jump rate (which is also predicted by the harmonic classical theory of solid state diffusion [25]) is justified for room temperature ($T = 300$ K) and above. Consequently, the qualitative behaviour of the rate as a function of temperature found for high temperatures $T > 300$ K is also valid for room temperature.

The numerical simulations presented in this paper are used to test the validity of different preexponential factors and to answer the question whether the "static" activation barrier of eq. (18) is in agreement with the dynamical value resulting from the simulations.

5. Results

Eight extended simulation series with model II were carried out independently with different randomly chosen initial kinetic energy values of the dipoles. The temperature was calculated from the total kinetic energy of the system. In each series the first 1000 integration steps with time intervals of $\Delta t = 2.5 \times 10^{-15}$ s were performed without the ion in the pore in order to obtain an equilibrium energy distribution between the pore dipoles. Then the ion was allowed to migrate in the model pore. No external field was applied, so that there was no preferred diffusion direction. The accuracy of the integration was tested by calculating the total energy of the system after each integration step. The energy was found to remain constant within 0.3 ‰ of the initial value during the whole simulation period. Furthermore, for one set of initial conditions the simulation was repeated using smaller time increments ($\Delta t = 1.25 \times 10^{-15}$ s instead of 2.5×10^{-15} s). It was found that this reduction at Δt had no influence on the ion trajectory. It was also tested whether the

length of the channel segment was sufficient in order to avoid self-interaction in the system due to the periodic boundary conditions. This is a particularly important point in all molecular dynamics simulations involving long-range Coulombic interactions. For this purpose one simulation was carried out with an increased length of the dipolar array (48 dipoles instead of 30). It was found that neither the general appearance of the ion trajectory nor the jump frequency was affected by increasing the length of the elementary unit.

The results of the simulation series are shown in fig. 5. It is seen that, in particular at low temperatures, the ion spends extended periods oscillating back and forth in a trapping site until it jumps to an adjacent site. The average oscillation frequency ν_0 was found to be nearly temperature independent ($\nu_0 = 2.2 \times 10^{12}$ s^{-1} with a variation of less than 7% in the temperature range between $T/\Theta_0 = 10$ and $T/\Theta_0 = 60$). This temperature range was chosen in order to reduce the ratio of ion vibration (10^{12}–10^{13} s^{-1}) at one site to the frequency of jumps over the barrier ($\sim 10^7$ s^{-1} at 300 K). At high temperatures relatively long jumps (over several sites) occasionally occur. The long jumps, however, do not influence the calculated jump probability w [eq. (8)] since neither N nor N_{jump} are expected to be influenced by the jump length. Moreover, an analysis of jump frequency as a function of jump length shows a sharp maximum of jumps between adjacent sites, as demonstrated in fig. 6. From the results of the dynamical calculations the jump probability w [eq. (8)] may be obtained. In fig. 7a, ln w is plotted as a function of Θ_0/T. It is seen that ln w is a linear function of $1/T$ within the estimated errors over a considerable temperature range, as predicted by eq. (19). Using eq. (19), the activation energy was determined to be $E_a = 0.334$ eV. The preexponential factor $A(T)$ in the relation $w = A(T)\exp(-E_a/kT)$ is found to be independent of temperature. This is more clearly demonstrated in figs. 7b and 7c where ln $(w \cdot T^{1/2})$ and ln $(wT^{-1/2})$ are plotted versus Θ_0/T corresponding to a preexponential factor $A(T)$ proportional to $T^{-1/2}$ and $T^{1/2}$, respectively. A $T^{1/2}$ behaviour is found for example for insterstitial diffusion in Debye solids [26–28] whereas if mainly the kinetic energy of the ion is coupled to the lattice motion of the dipoles also a $T^{1/2}$ proportional prefactor is possible as has been demonstrated by Fong [29]. It can be seen that neither in fig. 7b nor in fig. 7c do the results

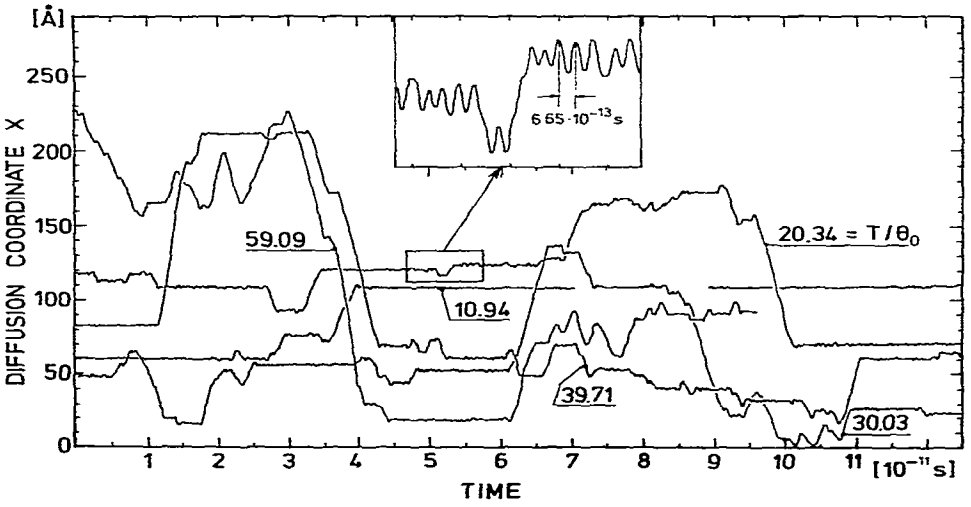

Fig. 5. Trajectories of ion migration in a helical channel of infinite length with antiparallel arrangement of dipoles (model II, fig. 3), obtained from dynamical simulations at five different temperatures ($\theta_0 = 103.2$ K). The following set of model parameters has been used: $r = 2.5$ Å, $a = h/3 = 4$ Å, $d = 1.128$ Å, $m = 1.063 \times 10^{-22}$ g, $q = 0.25\, e_0$, $D_r = 1.08 \times 10^{-18}$ J, $\phi_i^0 = 70°$, $M = 3.82 \times 10 \times 10^{-23}$ g, $Q = e_0 = 4.803 \times 10^{-10}$ e.s.u. The temperature was calculated from the total kinetic energy of the system, as specified by the initial conditions. Small oscillations arise from vibration of the ion in the trapping sites.

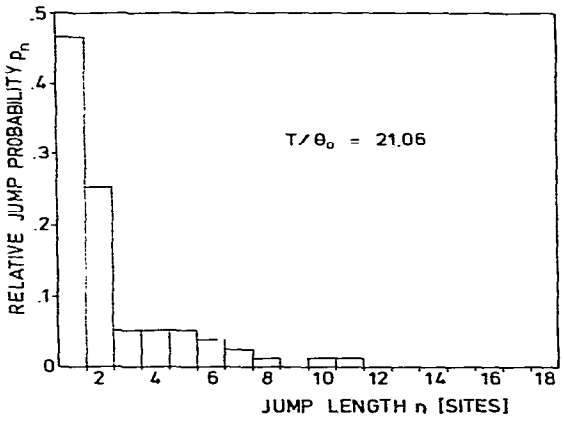

Fig. 6. Relative probability p_n of jumps of a given length at $T/\Theta_0 = 21.06$. p_n is the number of jumps to the nth site from the starting site, divided by the total number (N_{jump}) of jumps. At all temperatures (T/Θ_0 between 10 and 60) the distribution was found to have a maximum for jumps to the adjacent site ($n = 1$).

of the numerical experiments fall on a straight line within the error limits. As the fitting of the results with different temperature-dependent forms of the pre-exponential factor is rather sensitive, we can conclude that only the linear fit (fig. 7a) agrees satisfactorily with the simulation results, and that the pre-

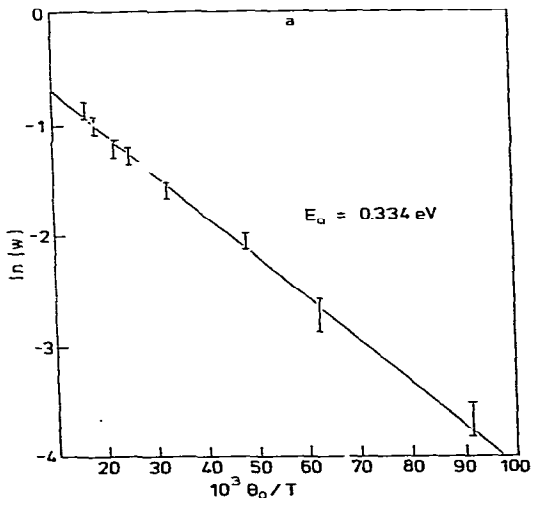

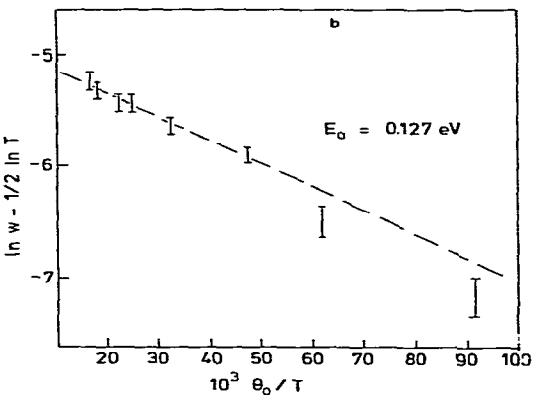

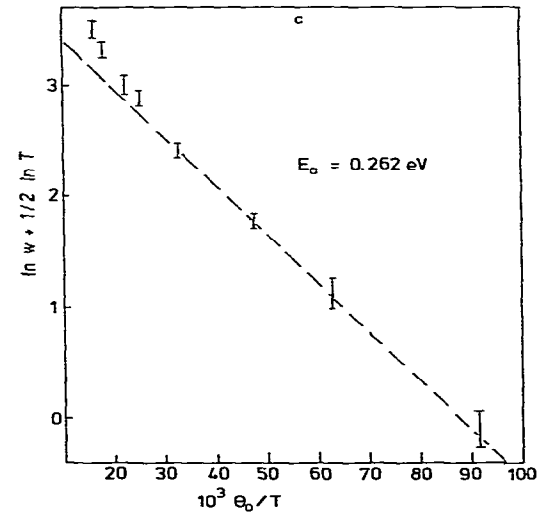

Fig. 7. Arrhenius plot of the jump probability w, as obtained from the results of the dynamical simulation, using eq. (8). Parameter values as in fig. 5. The statistical errors (indicated by bars) have been estimated from eq. (10). Different pre-exponential factors $A(T)$ have been used in the relation $w = A(T)\exp(-E_a/kT)$: a). $A(T) = \text{const.}$; b). $A(T) \propto T^{-1/2}$; c). $A(T) \propto T^{1/2}$.

exponential factor is indeed independent of temperature.

The observed value of the activation energy, $E_a = 0.334$ eV, can be compared with the predictions of rate theory. According to eq. (18), E_a should be approximately equal to the barrier height V_0, since the

quantum correction $h\nu_0/2 \approx 0.0045$ eV is negligible. As will be shown in the following, different theoretical values of V_0 have to be considered depending on the definition of the procedure by which the potential energy of the ion in the channel is evaluated. The most obvious definition of barrier height V_0 is based on the adiabatic potential of the ion which is obtained as the difference of a saddle point and a minimum in the f-dimensional energy surface as a function of the ion migrational coordinate and all dipole coordinates. (For the numerical calculation of the adiabatic potential, the ion is positioned at point x with all dipoles having the initial orientation $\phi_i = \phi_i^0$. The integration of the equations of motion is then started and after each time step the velocities of the dipoles are set to zero. This procedure ensures fast convergence towards the equilibrium conformation). The adiabatic potential which is obtained in this way is represented in fig. 3c. It is seen that the adiabatic barrier height is 0.505 eV, considerably larger than the observed activation energy (E_a = 0.334 eV). This means that at T = 300 K (kT = 0.026 eV) the actual transport rate is 1×10^3 times higher than the rate predicted on the basis of the adiabatic barrier height.

When the ion attempts to leave the trapping site, the ligand system may not be able to adjust sufficiently fast to the movement of the ion (as was assumed in the definition of the adiabatic potential). It is therefore useful to consider a second type of potential function which applies to the case that the ion is located in the trapping site and that the ligand system is held fixed in the resulting polarized equilibrium state (T = 0). This potential which is shown in fig. 8 would be "seen" by the ion during an "infinitely" fast jump out of the trapping site. The barrier for a jump to an adjacent site is 0.480 eV which is again higher than E_a. With increasing distance from the trapping site the barrier height approaches a limiting value of 0.350 eV.

This limiting value should be identical with the barrier height corresponding to the equilibrium conformation of the ligand system in the absence of the ion, i.e. the conformation which is assumed by the ligand system at T = 0 under the combined influence of dipole-dipole interactions and torsional forces. The potential function corresponding to this case is represented in fig. 3b.

The barrier height in this case was found to be V_0^{eq} = 0.350 eV which agrees with the limiting value for large distances mentioned above. The asymptotic value V_0^{eq} was already reached within 0.005 eV at the fourth site from the location of the ion. This result represents a further check that the length of the elemen-

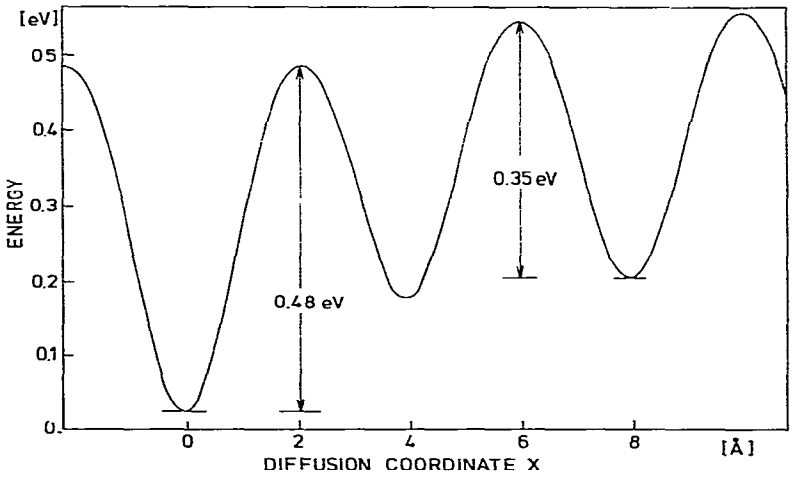

Fig. 8. Static potential energy for an ion jumping out of the trapping site at x = 0 at "infinite" velocity. The potential was calculated assuming that the ion is located in the trapping site and that the ligand system is held fixed in the resulting polarized equilibrium state (T = 0). With increasing distance from the trapping site the barrier height approaches a value of 0.350 eV.

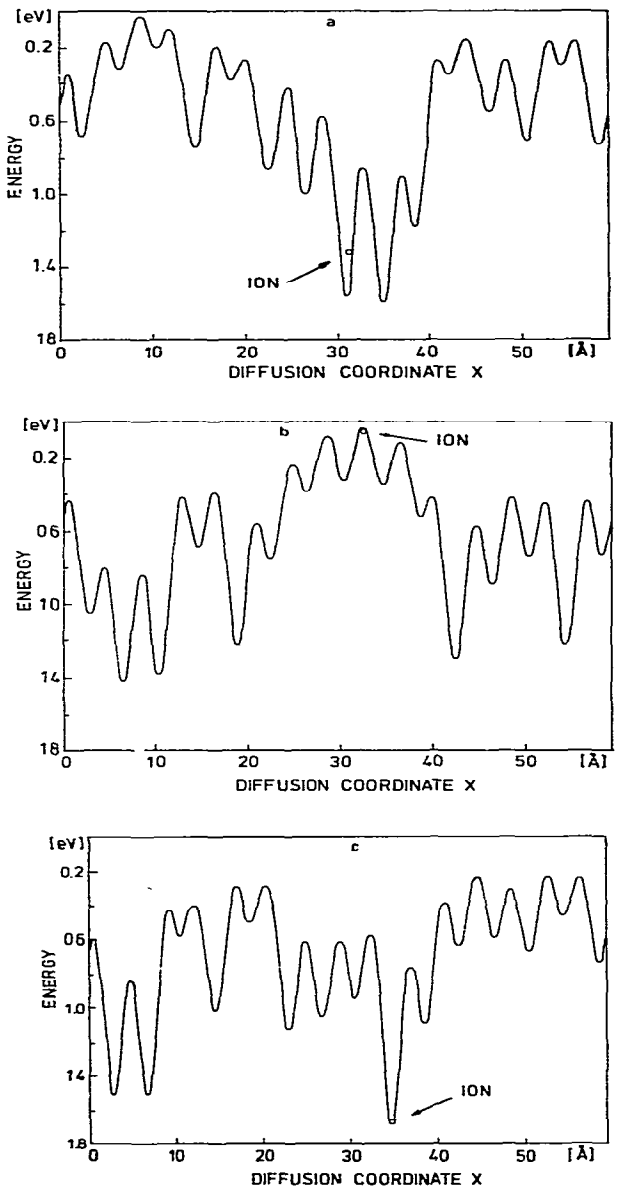

Fig. 9. Instantaneous energy profile of the ion in the channel at three consecutive times t during simulation at $T/\theta_0 = 60.19$. Upper profile: $t = 0$; middle profile: $t = 1.0$ ps; lower profile: $t = 1.5$ ps. The location and the energy of the ion is indicated in each case. The parameter values were the same as in fig. 5.

tary unit of the dipolar array is sufficient in order to avoid self-interaction.

In fig. 9 the instantaneous potential profile of the ion along the channel axis is given for three consecutive times before, during, and after a jump over a barrier. This representation clearly shows the large fluctuation in the shape of the potential curve which result from fluctuations in the conformation of the ligand system.

6. Discussion

In this molecular dynamics study of ion transport in membrane we have investigated the dynamical properties of a simple model which contains some of the essential features of transmembrane ion channels, namely, the presence of a ligand system which interacts electrostatically with the ion and which is deformable and able to transmit thermal fluctuations of kinetic energy to the ion. The first results which we report here mainly concern the general form of ion trajectories and the temperature dependence of rate constants: an analysis of the influence of other parameters, such as mass of the ion, geometry and flexibility of the ligand system and effects of non-coulombic terms in the interaction energy should be included in further studies. The ion trajectories obtained from the simulation clearly exhibit the theoretically expected oscillatory behaviour of the ion in the trapping site, i.e., the ion vibrates many times back and forth before it leaves the site and jumps over the barrier. As the observed oscillation frequency ν_0 is virtually temperature independent, the strong increase of transport rate with temperature results almost exclusively from the Arrhenius-type exponential dependence of jump probability on $1/T$. The interesting phenomenon of multiple jumps which mainly occur at higher temperatures probably depends on the strength of dynamical coupling between the motions of the ion and the ligand groups. It may be expected that changing the model parameters in such a way as to increase the efficiency of momentum transfer would reduce the probability of multiple jumps. (It should be noted that the efficiency of momentum transfer between ion and ligand groups does not merely depend on the depth of the energy wells: in a rigid ligand system momentum exchange is inefficient even if the activa-

tion barriers for ion movement are high).

From ν_0 and the jump probability w, the jump frequency $\nu = \nu_0 w$ may be calculated. Extrapolation to 300 K according to fig. 7a yields a jump frequency of $\nu = 5.3 \times 10^6\ s^{-1}$. Transport rates of comparable order of magnitude (10^7–$10^8\ s^{-1}$) have been observed in the gramicidin channel and ion channels of nerve membranes [3,8]. Using eq. (6) the diffusion coefficient D of the ion in the channel may be obtained. This gives (with a = 4Å) $D = 8.4 \times 10^{-9}\ cm^2\ s^{-1}$, a value which is about 10^3 times smaller than the diffusion coefficient of a free sodium ion in water.

An important result of this study is the fact that the observed activation energy E_a is considerably smaller than the height of the energy barrier V_0, calculated from the model. This discrepancy between E_a and V_0 is found irrespective whether in the calculation of V_0 the jump of the ion out of the trapping site is treated as slow or as fast compared with the relaxation of the ligand system. (A closer agreement is observed between the activation energy, $E_a = 0.334$ eV, and the barrier height corresponding to the equilibrium conformation of the ligand system, $V_0^{eq} = 0.350$ eV, but this coincidence is probably fortuitous). An explanation for the finding that the observed transport rate is much larger than predicted from the barrier height is probably given by the fact that at non-zero temperature the conformation of the ligand system is subjected to thermal fluctuations (compare fig. 9). This in turn gives rise to fluctuations of barrier height [31]. An ion will preferentially jump over a barrier when the barrier is low, which means that those ligand conformations with small barrier heights are most significant for ion transport in the channel.

An inherent difficulty in the application of molecular dynamics techniques to ion transport in membranes is the wide separation of time scales of the different processes [10,32]. Whereas the oscillation frequency of the ion in a trapping site is of the order of 10^{12}–$10^{13}\ s^{-1}$, the frequency of jumps over a barrier at room temperature may be only $10^7\ s^{-1}$ or even longer. This means that very long trajectories are required in order to observe a statistically significant number of the events of interest. In order to circumvent this problem of infrequent events, we have carried out the simulation at elevated temperatures. This procedure is based on the fact that the frequency of oscillation in the trapping site is only weakly temperature-dependent, whereas the frequency of jumps over a barrier depends exponentially on $1/T$. The jump probability w obtained at large values of T may then be extrapolated to lower temperatures using the theoretically predicted exponential relationship between w and $1/T$ [eq. (19)]. The main justification for this extrapolation results from the fact that the plot of $\ln w$ versus θ_0/T (fig. 7a) is already linear at the highest temperatures used in this study ($T/\theta_0 \leqslant 60$) and remains linear towards lower temperatures, in agreement with eq. (19). Deviations from eq. (19) do occur at still higher temperatures ($\ln w$ does not go to zero for $\theta_0/T \to 0$ in fig. (7a)), but there is no reason to assume that the linear relationship between $\ln w$ and $1/T$ should break down at lower temperatures. This extrapolation method presumably can be applied also in other dynamical simulations of other systems.

We like to point out that the present calculations are based on a simple model pore including only a few empirical parameters like electrostatically ion-dipole interaction and the geometry of the pore. With this simple model the mean features of the ion transport in protein channels can sufficiently be described. It is clear that the occurrence of other particles in the pore (like water molecules) and the mechanism of entering into and exciting from the channel will influence the dynamical behaviour of our model system. Such effects are currently under study.

Acknowledgement

We like to thank M. Kloeffler and H.U. Raab for some comments, Dr. E.E. Polymeropoulos for critically reading the manuscript, H.A. Schmaltz for carefully drawing the figures and B. Brickmann for technical assistance.

References

[1] Ion permeation through membrane channels, eds. C.F. Stevens and R.W. Tsien, Membrane transport processes, Vol. 3, (Raven Press, New York, 1979).

[2] D.W. Urry, Proc. Natl. Acad. Sci. 68 (1971) 672.

[3] S.B. Hladky and D.A. Haydon, Biochim. Biophys. Acta 274 (1972) 294.

[4] E. Bamberg and P. Läuger, J. Membrane Biol. 11 (1973) 177.

number of the events of interest. In order to circumvent this problem of infrequent events, we have carried out the simulation at elevated temperatures. This procedure is based on the fact that the frequency of oscillation in the trapping site is only weakly tempera-

[2] D.W. Urry, Proc. Natl. Acad. Sci. 68 (1971) 672.

[3] S.B. Hladky and D.A. Haydon, Biochim. Biophys. Acta 274 (1972) 294.

[4] E. Bamberg and P. Läuger, J. Membrane Biol. 11 (1973) 177.

[5] G. Eisenman, J. Sandblom and E. Neher, Biophys. J. 22 (1978) 307.
[6] S. Weinstein, B.A. Wallace, E.R. Blout, J.S. Morrow and W. Veatch, Proc. Natl. Acad. Sci. 76 (1979) 4230.
[7] O. Andersen and J. Procopio, Acta Physiol. Scand. Suppl. 481 (1980) 27.
[8] C.M. Armstrong, Quat. Rev. Biophys. 7 (1975) 179.
[9] W.W. Wood and J.J. Erpenback, Ann. Rev. Phys. Chem. 27 (1976) 319.
[10] J. Kushick and B.J. Berne, in: Modern theoretical chemistry, Vol. 6, ed. B.J. Berne (Plenum Press, New York, 1977) pp. 41–63.
[11] Computer modelling of matter, ed. P. Lykos, ACS Symposium Series 86 (American Chemical Society, Washington, 1978).
[12] D.G. Levitt, Biophys. J. 13 (1973) 186.
[13] D.G. Levitt and G. Subramanian, Biochim. Biophys. Acta 373 (1974) 132.
[14] Y. Koyama and T. Shimanouchi, in: Peptides, polypeptides and proteins, eds. E.R. Blout, F.A. Bovey, M. Goodman and N. Lotan, (John Wiley, New York, 1974) pp. 396–418.
[15] B.J. Zwolinski, H. Eyring and C.E. Reese, J. Phys. Chem. 53 (1949) 1426.
[16] J.W. Woodbury, in chemical dynamics, Papers in Honor of Henry Eyring, ed. J. Hirschfelder (John Wiley and Sons, New York, 1971) pp. 601–617.
[17] P. Läuger, Biochim. Biophys. Acta 311 (1973) 423.
[18] B. Hille, J. Gen. Physiol. 66 (1975) 535.
[19] See, for example, W. Jost, Diffusion in solids, liquids and gases (Academic Press, New York, 1952).
[20] See, for example, M. Rosenblatt, Random processes (Springer, New York, 1970).
[21] H. Eyring, J. Chem. Phys. 4 (1936) 283.
[22] R.E. Powell, W.E. Roseveare and H. Eyring, Ind. Eng. Chem. 33 (1941) 430.
[23] J.F. Kincaid, H. Eyring and A.E. Stearn, Chem. Res. 28 (1941) 301.
[24] See, for example, T.L. Hill, Statistical thermodynamics, (Addison-Wesley, Reading, 1962) p. 151 f.
[25] W.M. Franklin, in: Diffusion in solids, eds. A.S. Novick and J.J. Burton (Academic Press, New York, 1975) p. 50.
[26] A.M. Stoneham, J. Phys. F.: Metal Phys. 2 (1972) 417.
[27] C.P. Flynn and A.M. Stoneham, Phys. Rev. B1 (1976) 3966.
[28] C.P. Flynn, Comm. Solid State Phys. 3 (1971) 159.
[29] F.K. Fong, Theory of molecular relaxation (John Wiley, New York, 1975) Chapter 7.
[30] J.O. Hirschfelder, C.F. Curtiss and B.B. Bird, Molecular theory of gases and liquids (John Wiley and Sons, New York, 1954) p. 664.
[31] P. Läuger, W. Stephan and E. Frehland, Biochim. Acta (in press).
[32] C.H. Bennett, in: Algorithms for chemical computations, ed. R.E. Christoffersen, ACS Symposium Series 46 (American Chemical Society, Washington, D.C., 1977) pp. 63–97.